

Crossing contours in the interacting boson approximation (IBA) symmetry triangle

E. A. McCutchan and R. F. Casten

WNSL, Yale University, New Haven, Connecticut 06520-8124, USA

(Received 14 August 2006; published 9 November 2006)

Constant contours of basic observables are discussed in the context of the interacting boson approximation (IBA) symmetry triangle. Contours that exhibit orthogonal crossing within the triangle are presented as a method for determining a set of parameter values for a particular nucleus and trajectories for isotopic chains. A set of contours that highlights a class of nuclei that are outside the two-parameter IBA-1 Hamiltonian space is also presented.

DOI: [10.1103/PhysRevC.74.057302](https://doi.org/10.1103/PhysRevC.74.057302)

PACS number(s): 21.10.Re, 21.60.Fw

Collectivity in low-energy nuclear structure is traditionally described relative to particular models. At a very basic level, the structure of an even-even nucleus can be understood by comparing its properties to the three traditional benchmarks of structure, the harmonic vibrator, deformed symmetric rotor, or γ -unstable shape. However, most nuclei are known to exhibit structures intermediate between these shapes and a better description can usually be obtained with a variable parameter model. The task then becomes to determine the model Hamiltonian parameter values relevant to a specific nucleus.

One of the standard approaches for extracting parameter values appropriate for a particular nucleus is to consider contour plots of basic observables. The purpose of this Brief Report is to describe a simplified approach using such contours to pinpoint parameters in the framework of the interacting boson approximation (IBA) model [1]. These contours will be analyzed as to their effectiveness in determining a unique set of parameters. A simple contour is presented that exhibits orthogonal crossing with most others. This approach is then discussed as a method for roughly determining the trajectories of isotopic chains in the IBA triangle. Knowledge of these trajectories gives an understanding of what collective behavior nuclei exhibit and thus provides a challenge to microscopic theories to explain this behavior in terms of the underlying nucleon motion and interactions.

Calculations of contours of observables are performed in the framework of the IBA-1 using the extended [2] consistent Q [3] formalism (ECQF) with the Hamiltonian [4,5],

$$H(\zeta) = c \left[(1 - \zeta) \hat{n}_d - \frac{\zeta}{4N_B} \hat{Q}^x \cdot \hat{Q}^x \right], \quad (1)$$

where

$$\hat{Q}^x = (s^\dagger \tilde{d} + d^\dagger s) + \chi (d^\dagger \tilde{d})^{(2)} \quad (2)$$

and $\hat{n}_d = d^\dagger \tilde{d}$.

The Hamiltonian of Eq. (1) involves two parameters, ζ and χ (c is a scaling factor). The boson number N_B is given by half the number of valence protons and neutrons, each taken separately relative to the nearest closed shell.

The parameter space for this Hamiltonian is conveniently represented by a triangle [6] with one IBA dynamical symmetry at each vertex, as illustrated in Fig. 1. In this parametrization, the three symmetries are given by $\zeta = 0$, any χ for $U(5)$, $\zeta = 1$, $\chi = -\sqrt{7}/2$ for $SU(3)$, and $\zeta = 1$, $\chi = 0$

for $O(6)$. Transition regions between the three symmetries can be described by numerical diagonalizations of the above Hamiltonian for intermediate parameter (ζ , χ) values.

Contour plots are generally illustrated in a Cartesian space as a function of the parameters (in this case ζ and χ). To allow for a better visualization of how the contours evolve between the three limiting symmetries, they will be plotted directly into the IBA symmetry triangle by converting the parameters ζ and χ of Eq. (1) into radial and angular coordinates (ρ , θ) by [7]

$$\begin{aligned} \rho &= \frac{\sqrt{3}\zeta}{\sqrt{3}\cos\theta_\chi - \sin\theta_\chi} \\ \theta &= \frac{\pi}{3} + \theta_\chi, \end{aligned} \quad (3)$$

where $\theta_\chi = (2/\sqrt{7})\chi(\pi/3)$. In this coordinate system, θ ranges from 0° to 60° and ρ acts as a standard radial coordinate ranging from 0 to 1.

The technique of using contour plots of observables to extract IBA parameter values is certainly not new. The first example of this approach within the framework of the IBA was outlined in the introduction of the consistent Q formalism [3] where contour plots of various observables as a function of N_B and χ were used to determine parameter values appropriate for well-deformed nuclei. Since then, subsequent IBA investigations (see, for example, Refs. [2,8,9]) have used the same or similar (such as ζ versus χ) contour plots to fit individual nuclei and/or isotopic chains. We begin by analyzing contour plots similar to those given in these previous studies and investigate their effectiveness in extracting appropriate parameter values and then move on to describe a new class of contours.

There are numerous experimental observables that can provide insight into nuclear structure. Here, the focus is on the most basic observables and, hence, usually the best known experimentally, such as low-spin yrast energies, the energy of the first excited 0^+ state, and the energy of the quasi- 2_γ state. The methods presented here serve only as an estimate for parameter values and, certainly, a detailed interpretation of a nucleus would involve considering a wider class of relevant experimental observables.

Starting with the $R_{4/2} \equiv E(4_1^+)/E(2_1^+)$ energy ratio, IBA calculations were performed for a mesh of ζ and χ values and parameter sets giving constant values of $R_{4/2}$ were determined.

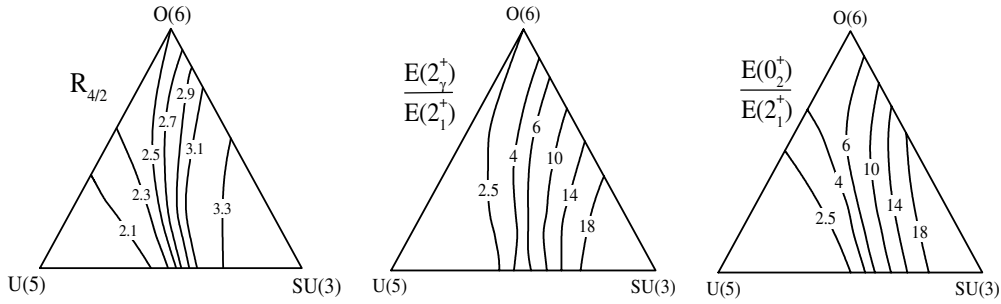


FIG. 1. Symmetry triangle of the IBA with contours of constant values of energy ratios of basic observables, $R_{4/2}$ (left), $E(2_{\gamma}^+)/E(2_1^+)$ (middle), and $E(0_2^+)/E(2_1^+)$ (right). Calculations are for $N_B = 10$.

The resulting $R_{4/2}$ contours are given in Fig. 1 (left). The region around $U(5)$ gives $R_{4/2}$ values close to the vibrational limit. With increasing ζ , $R_{4/2}$ increases, approaching the axially symmetric rotational value of 3.33 in the $SU(3)$ vertex. Clearly, the $R_{4/2}$ energy ratio alone does not constrain the parameter values, because each $R_{4/2}$ contour traces out an entire locus of parameter values in the triangle, cutting more or less vertically through the triangle.

Similar contours can be constructed for additional energy ratios, such as $E(0_2^+)/E(2_1^+)$ and $E(2_{\gamma}^+)/E(2_1^+)$, as also shown in Fig. 1. Their evolution in the triangle represents the change in character from multiphonon structure in $U(5)$ to intrinsic excitations in $SU(3)$ or $O(5)$ excitations in $U(6)$. Both sets of contours display a similar evolution in the triangle, values of 2.0 close to the $U(5)$ region that increase with increasing deformation, passing more or less vertically through the triangle and they also resemble the behavior of the $R_{4/2}$ contours. These observables are therefore usually not useful in pinpointing structure because they do not provide a unique intersection with $R_{4/2}$ over most of the triangle. In general, energies of individual low-lying, positive-parity states (normalized to the 2_1^+ energy) trace out similar vertical paths through the triangle.

Contours with more horizontal trajectories can, however, be obtained by combining the energies of different intrinsic states. One such contour used in Refs. [2,8,10] is given by

$$R_{02} = \frac{E(0_2^+)}{E(2_{\gamma}^+) - E(2_1^+)} \quad (4)$$

and is illustrated in Fig. 2 (left). Although this contour provides horizontal trajectories for some regions, there is still a large

region (contours which correspond to R_{02} values ~ 1.6 – 2.4) where they follow a similar path as say, $R_{4/2}$.

Here, we propose a new class of contours, involving a *difference* of energies of intrinsic excitations. The most useful case of this is

$$R_{0\gamma} = \frac{E(0_2^+) - E(2_{\gamma}^+)}{E(2_1^+)}, \quad (5)$$

which is illustrated in Fig. 2 (right). These contours are sensitive to the relative movement of the 0_2^+ and 2_{γ}^+ states with deviations from $U(5)$ (degenerate) or $SU(3)$ (β, γ vibrations almost degenerate) and are roughly perpendicular to the $R_{4/2}$ contours for almost all regions of the triangle, apart from a small region close to the $O(6)$ vertex. Furthermore, $R_{0\gamma}$ has the somewhat unique property that it separates the triangle into two distinct regions. For $E(0_2^+) < E(2_{\gamma}^+)$ a nucleus would be described by parameters along or near the bottom leg of the triangle, whereas if $E(0_2^+) > E(2_{\gamma}^+)$ the parameter space is constrained to the upper region of the triangle. We return to the significance of this boundary later.

The intersection of a $R_{0\gamma}$ contour with a $R_{4/2}$ contour [or similarly a $E(0_2^+)/E(2_1^+)$ or $E(2_{\gamma}^+)/E(2_1^+)$ contour] provides a unique point of parameter values for describing a particular nucleus. To elucidate the evolution of an isotopic chain in the IBA triangle, the progression of the above contours with varying boson number must also be considered. The contours for $R_{4/2}$ and $R_{0\gamma}$ will be used as examples although the same overall trends apply to other observables. A comparison of the $R_{4/2}$ and $R_{0\gamma}$ contours is given in Fig. 3 for boson numbers 6 and 16.

Several features become immediately obvious when comparing the results for different boson numbers in Fig. 3. For $R_{4/2}$, the vibrational region up to $R_{4/2} \sim 2.5$ is very similar regardless of boson number. For increasing boson number, the increase in $R_{4/2}$ across the transition region becomes more rapid, indicated by a compression of the contours. This corresponds to the spherical to deformed phase transition region discussed in Refs. [11,12]. For large boson number, the area corresponding to rotational values of $R_{4/2} \sim 3.3$ extends further into the interior of the triangle.

For $R_{0\gamma}$, the contour corresponding to a near degeneracy between the 0_2^+ state and the 2_{γ}^+ state does not vary significantly with boson number. Above and below the contour of $R_{0\gamma} \sim 0$, the contours follow a similar pattern. The main difference is the overall scales. For example, in the region close to $O(6)$,

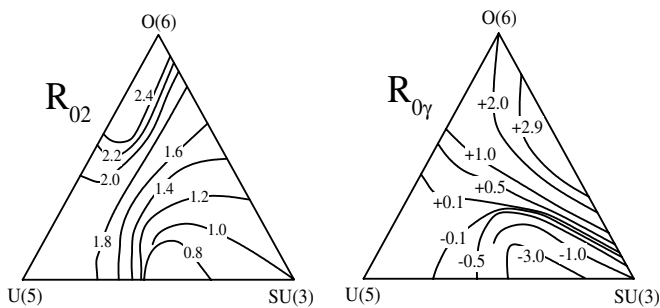


FIG. 2. Contours of constant values of the energy ratios $R_{02} \equiv E(0_2^+)/[E(2_{\gamma}^+) - E(2_1^+)]$ (left) and $R_{0\gamma} \equiv [E(0_2^+) - E(2_{\gamma}^+)/E(2_1^+)]$ (right) in the IBA triangle. Calculations are for $N_B = 10$.

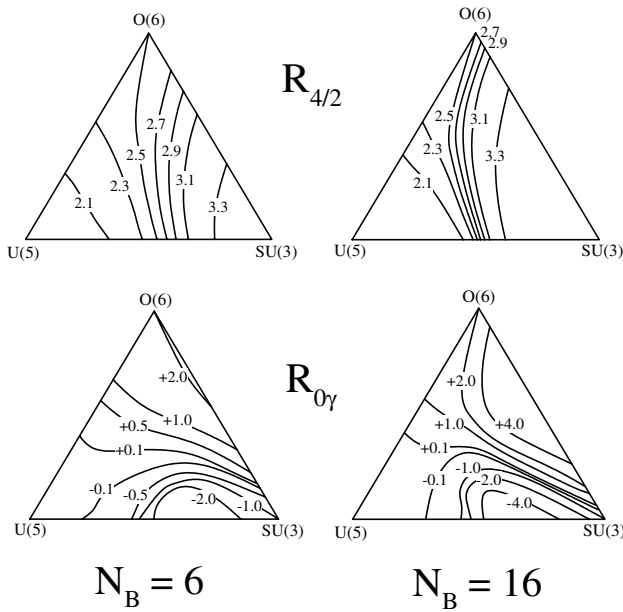


FIG. 3. Contours of constant values of the energy ratios $R_{4/2}$ (top) and $R_{0\gamma}$ (bottom) in the IBA triangle for $N_B = 6$ (left) and $N_B = 16$ (right).

along the $O(6)$ - $SU(3)$ leg of the triangle, the $R_{0\gamma}$ ratio is ~ 2 for $N_B = 6$ and grows to values > 4 for $N_B = 16$.

The near constancy of the contour $R_{0\gamma} \sim 0$ independent of boson number is interesting. In fact, it was recently shown [13] that a degeneracy of the 0_2^+ and 2_2^+ states corresponds to a nearly regular region amid the basically chaotic interior region of the triangle. Thus the contour $R_{0\gamma} \sim 0$, which divides the triangle according to whether the 0_2^+ state is above or below the 2_2^+ state, also marks the unique locus of regular behavior within the triangle. Further study of structure along this locus would be very interesting.

Now equipped with a set of orthogonal contours, the evolution of an isotopic chain within the IBA triangle can be determined. Taking the Dy isotopic chain as an example, the experimental values of $R_{4/2}$ and $R_{0\gamma}$ are plotted in Fig. 4. The $R_{4/2}$ energy ratio rises quickly for neutron numbers between 88 and 92 and then remains relatively constant around 3.3 for larger neutron numbers. The sharp rise in $R_{4/2}$ suggests that the beginning of the isotopic chain ($N = 88$ – 92) evolves close to the $U(5)$ - $SU(3)$ leg of the triangle because this is where $R_{4/2}$ undergoes the most rapid increase. This agrees with the $R_{0\gamma}$ ratio that experimentally starts out slightly negative and approaches zero before turning sharply positive. Negative values of $R_{0\gamma}$ can be obtained only in the IBA near the $U(5)$ - $SU(3)$ leg of the triangle. For $N \geq 94$, the relatively constant $R_{4/2}$ value (~ 3.3) and large boson numbers constrain the trajectory to a large region of the right-hand side of the triangle. The exact trajectory can be determined by considering the $R_{0\gamma}$ ratio that experimentally goes through zero and then becomes increasingly more positive. This behavior can be followed in the triangle by turning away from the $U(5)$ - $SU(3)$ leg of the triangle and approaching the $O(6)$ - $SU(3)$ leg. A schematic representation of this trajectory is illustrated in the inset of Fig. 4.

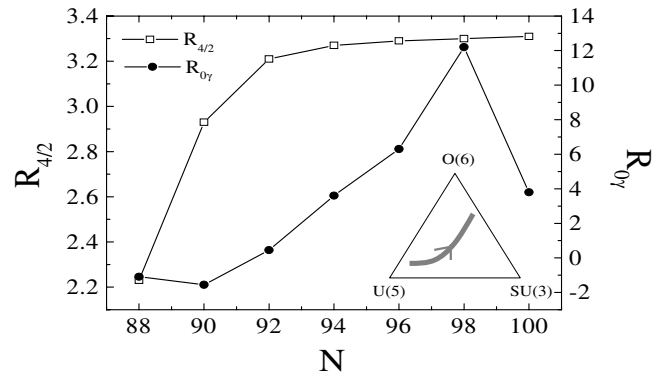


FIG. 4. Values of the energy ratios $R_{4/2}$ (open squares) and $R_{0\gamma}$ (solid circles) for the Dy isotopic chain. The inset gives a schematic representation of the trajectory of the Dy isotopic chain in the IBA triangle.

The crossing of the $R_{4/2}$ contours and the $R_{0\gamma}$ contours can be useful in some cases but misleading in others. Careful study of these and other contours involving energy differences of intrinsic states reveals a class of nuclei that cannot be fit with the ECQF Hamiltonian. To illustrate this, consider $N_B = 16$, where there is no consistent set of parameters to describe nuclei with $R_{4/2}$ values < 2.5 and $R_{0\gamma}$ values > 4.0 . A less obvious case occurs for $R_{0\gamma} \sim 0$, because this contour intersects all of the $R_{4/2}$ contours, seeming to imply that any nucleus with a collective $R_{4/2}$ and $R_{0\gamma} \sim 0$ can be fit with the ECQF Hamiltonian. However, problems can arise because the overall scale of $E(0_2^+)$ and $E(2_2^+)$ are lost when the numerator of $R_{0\gamma}$ is close to zero and so, although $R_{4/2}$ and $R_{0\gamma}$ can be reproduced, there is no guarantee that the ratios $E(0_2^+)/E(2_1^+)$ or $E(2_2^+)/E(2_1^+)$ are well described. To illustrate the issue consider contours involving the difference between one of the above two intrinsic states and the ground-state band

$$R_{06} = \frac{E(0_2^+) - E(6_1^+)}{E(2_1^+)} \tag{6}$$

$$R_{\gamma 6} = \frac{E(2_2^+) - E(6_1^+)}{E(2_1^+)}$$

illustrated in Fig. 5. In nuclei where $R_{0\gamma} \sim 0$, the ratios R_{06} and $R_{\gamma 6}$ will be nearly equal. For positive values and for

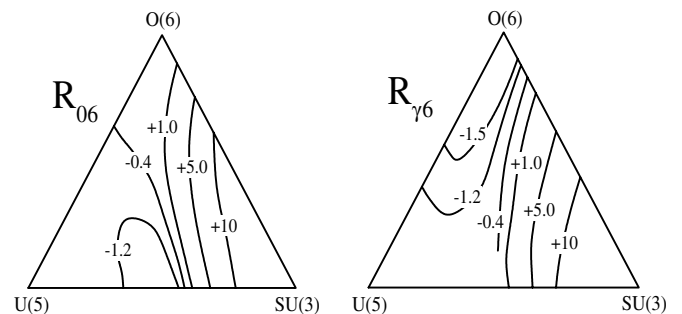


FIG. 5. Constant contours of the ratios R_{06} (left) and $R_{\gamma 6}$ (right) in the IBA triangle. Calculations are for $N_B = 10$.

negative values of R_{06} and $R_{\gamma 6}$ down to about -1.0 , the R_{06} and $R_{\gamma 6}$ contours intersect for $R_{06} = R_{\gamma 6}$ along the line of $R_{0\gamma} \sim 0$. However, for R_{06} and $R_{\gamma 6} < -1.0$, there is no intersection for $R_{06} = R_{\gamma 6}$, because these two contours form pockets in incompatible regions of the triangle; $R_{06} < -1.0$ along the $U(5)$ - $SU(3)$ leg and $R_{\gamma 6} < -1.0$ along the $U(5)$ - $O(6)$ leg. Therefore, for nuclei with $R_{0\gamma} \sim 0$ and both R_{06} and $R_{\gamma 6} < -1.0$, a consistent set of parameters cannot be obtained. That is, in nuclei where the 0_2^+ and 2_γ^+ levels are close lying, but both are well below the 6_1^+ level, no solution is possible with the ECQF IBA-1 Hamiltonian.

A survey of the available data identifies about 20 collective nuclei where $R_{0\gamma} \sim 0$ and both R_{06} , $R_{\gamma 6} < -1.0$ and thus lie outside the simple two-parameter IBA space. Some of these nuclei, $^{102-106}\text{Pd}$ and $^{110-120}\text{Cd}$, are known [14,15] to have additional degrees of freedom, such as intruder state 0^+ excitations. The inability of the IBA to reproduce the

basic properties of the other identified nuclei, $^{118-122}\text{Xe}$, $^{124-130}\text{Ba}$, and $^{130-136}\text{Ce}$, could also suggest additional degrees of freedom present in these nuclei. It would be interesting to study if the use of the most general IBA-1 Hamiltonian, as discussed in Refs. [16,17], could alleviate this problem.

In summary, we have discussed contours of basic observables within the IBA symmetry triangle in terms of their effectiveness for determining a unique set of parameter values particular for individual nuclei and/or isotopic chains. We identified a contour involving the difference between the 0_2^+ and 2_γ^+ states that gives orthogonal crossings with most other contours of basic observables and we observe a class of nuclei that cannot be fit with the two-parameter, ECQF Hamiltonian.

Valuable discussions with N. V. Zamfir and F. Iachello are acknowledged. This work was supported by U.S. DOE Department of Energy grant No. DE-FG02-91ER-40609.

-
- [1] F. Iachello and A. Arima, *The Interacting Boson Model* (Cambridge University Press, Cambridge, 1987).
- [2] P. O. Lipas, P. Toivonen, and D. D. Warner, Phys. Lett. **155B**, 295 (1985).
- [3] D. D. Warner and R. F. Casten, Phys. Rev. Lett. **48**, 1385 (1982).
- [4] V. Werner, N. Pietralla, P. von Brentano, R. F. Casten, and R. V. Jolos, Phys. Rev. C **61**, 021301(R) (2000).
- [5] N. V. Zamfir, P. von Brentano, R. F. Casten, and J. Jolie, Phys. Rev. C **66**, 021304(R) (2002).
- [6] R. F. Casten, in *Interacting Bose-Fermi Systems in Nuclei*, edited by F. Iachello (Plenum, New York, 1981), p. 1.
- [7] E. A. McCutchan, N. V. Zamfir, and R. F. Casten, Phys. Rev. C **69**, 064306 (2004).
- [8] W.-T. Chou, N. V. Zamfir, and R. F. Casten, Phys. Rev. C **56**, 829 (1997).
- [9] D. Bucurescu, G. Cata, D. Cutoiu, G. Constantinescu, M. Ivascu, and N. V. Zamfir, Z. Phys. A **324**, 387 (1986); **327**, 241(E) (1987).
- [10] M. K. Harder and K. T. Tang, Phys. Lett. **B369**, 1 (1996).
- [11] F. Iachello, N. V. Zamfir, and R. F. Casten, Phys. Rev. Lett. **81**, 1191 (1998).
- [12] R. F. Casten, Dimitri Kusnezov, and N. V. Zamfir, Phys. Rev. Lett. **82**, 5000 (1999).
- [13] J. Jolie, R. F. Casten, P. Cejnar, S. Heinze, E. A. McCutchan, and N. V. Zamfir, Phys. Rev. Lett. **93**, 132501 (2004).
- [14] M. Kadi, N. Warr, P. E. Garret, J. Jolie, and S. W. Yates, Phys. Rev. C **68**, 031306 (2003).
- [15] J. L. Wood, K. Heyde, W. Nazarewicz, M. Huyse, and P. van Duppen, Phys. Rep. **215**, 101 (1992).
- [16] A. Gómez, O. Castaños, and A. Frank, Nucl. Phys. **A589**, 267 (1995).
- [17] J. E. García-Ramos, J. M. Arias, J. Barea, and A. Frank, Phys. Rev. C **68**, 024307 (2003).